

Diagnostics of ballistic electrons in a dc/rf hybrid capacitively coupled discharge

Lin Xu,^{1,a)} Lee Chen,^{1,b)} Merritt Funk,¹ Alok Ranjan,¹ Mike Hummel,¹ Ron Bravenec,¹ Radha Sundararajan,¹ Demetre J. Economou,^{2,c)} and Vincent M. Donnelly^{2,d)}

¹Tokyo Electron America, Austin, Texas 78741, USA

²Department of Chemical and Biomolecular Engineering, Plasma Processing Laboratory, University of Houston, Houston, Texas 77204-4004, USA

(Received 6 October 2008; accepted 8 December 2008; published online 31 December 2008)

The energy distribution of ballistic electrons in a dc/rf hybrid parallel-plate capacitively coupled plasma reactor was measured. Ballistic electrons originated as secondaries produced by ion and electron bombardment of the electrodes. The energy distribution of ballistic electrons peaked at the value of the negative bias applied to the dc electrode. As that bias became more negative, the ballistic electron current on the rf substrate electrode increased dramatically. The ion current on the dc electrode also increased. © 2008 American Institute of Physics. [DOI: 10.1063/1.3062853]

Capacitively coupled plasmas (CCPs) are extensively used in the semiconductor industry for thin film etching and deposition. The direct current (dc)/radio frequency (rf) hybrid parallel-plate CCP etcher is powered with both dc and rf sources. Two configurations have been explored: dc and rf supplied to the same electrode^{1,2} or a negatively biased dc electrode facing a rf substrate electrode, where wafers are situated during plasma processing. These hybrid configurations can significantly alleviate the electron shading effect and preserve photoresist integrity.³⁻⁵ It is thought that a group of ballistic electrons (BEs) with relatively high energy and small angular divergence is responsible for these results.⁶ These BEs may start as secondary electrons (SEs) due to ion bombardment of the dc electrode. Secondaries are subsequently accelerated by the sheath adjacent to the dc electrode and enter the plasma. Because the collision mean free path is relatively low at very high energies, BE can traverse the bulk plasma without excessive gas-phase collisions and impact the substrate electrode or the semiconductor wafer.

Watanabe *et al.*⁷ superimposed a high energy electron beam on a conventional etcher. A rf induction coil was used to sustain an inductively coupled plasma while a rf-powered cathode immersed in the plasma was used to generate a BE beam directed toward a parallel plate substrate electrode.^{8,9} It was suggested that BEs from the beam reached the bottom of microscopic features on the wafer, reducing the net charge buildup and minimizing profile artifacts during oxide etch. In a practical plasma etcher, however, the substrate electrode is rf biased and this influences the energy and flux of electrons ultimately reaching the substrate. The bulk plasma properties may also be affected. For instance, in the dc/rf hybrid, a fraction of the BEs injected from the dc electrode could be trapped by the sheath voltage on the rf electrode. This electron “trapping” can conceivably lead to enhanced gas-phase ionization and higher plasma density.^{2,6} Measurement of the energy distribution of electrons impinging on a rf biased sub-

strate electrode and the corresponding modifications of the bulk plasma are crucial for understanding the behavior of the dc/rf hybrid etcher and the influence of BE on wafer processing.

A schematic of the dc/rf hybrid parallel-plate etcher used in this work is shown in Fig. 1. The reactor vessel was a 16 in. diameter, 18 in. high stainless steel cylinder. Power at 13.56 MHz was delivered through a matching network to an 8 in. diameter aluminum rf substrate electrode. The dc aluminum electrode (8 in. diameter) was 3 cm above the substrate electrode and had a showerhead for the distribution of Ar gas (99.999% purity). An LC filter blocked any 13.56 MHz rf signal on the dc electrode. However, an ~40 V peak-to-peak ripple at higher harmonics was still detectable. The back and side of both electrodes were covered with a ground shield. The large area ratio of the grounded surfaces, compared to the rf electrode surface, resulted in a high dc self-bias on the rf electrode with a concomitantly low plasma potential. The negative dc bias applied to the counter electrode should not affect that plasma potential. A 2300 l/s turbomolecular pump was used to evacuate the chamber and the system base pressure was routinely below 3×10^{-8} Torr.

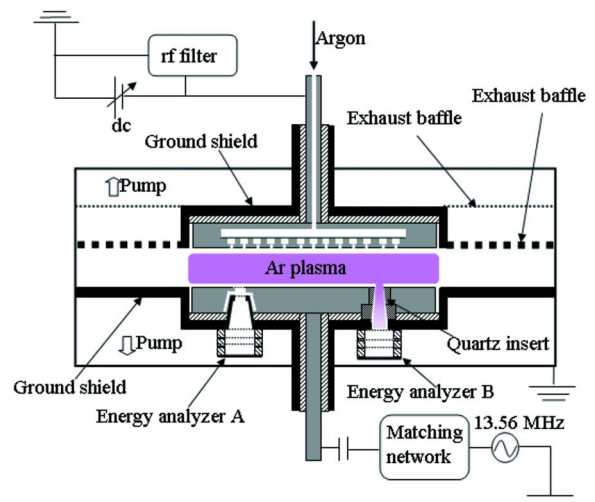


FIG. 1. (Color online) Schematic of the experimental setup used in the present work.

^{a)}Electronic mail: lin.xu@us.tel.com.

^{b)}Electronic mail: lee.chen@us.tel.com.

^{c)}Electronic mail: economou@uh.edu.

^{d)}Electronic mail: vmdonnelly@uh.edu.

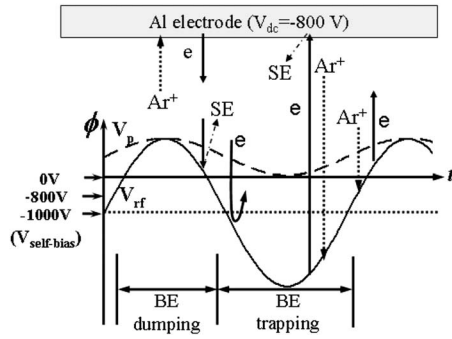


FIG. 2. Possible channels generating BEs in a dc/rf hybrid CCP reactor. Both ion and electron bombardments of the electrodes can lead to BE production.

Two apertures on the rf electrode at a radial distance of 1.5 in. on either side of the electrode axis were used to sample electrons. One aperture (7 mm diameter) was covered with a 20% transparency stainless steel mesh having 75 μm diameter holes at the same potential as the rf electrode. This aperture was used to sample electrons bombarding the rf electrode. Electrons entered analyzer A, housed below this aperture, with an acceptance angle of 25° . A cylindrical quartz insert having a 7 mm diameter entrance hole (not covered by mesh) was fitted on the other aperture. This hole tapered to 15 mm diameter over a length of 30 mm. The hole size was large enough for plasma to leak into the quartz insert, allowing analyzer B to sample bulk plasma electrons. The pressure behind the rf electrode was two orders of magnitude lower than the discharge pressure. Thus, collisions of electrons entering the analyzers could be neglected for a typical discharge pressure of 50 mTorr. Each energy analyzer consisted of three stainless-steel grids (all 80% transparent) and a current collector. The top grid was grounded and the middle grid was biased at +200 V (referenced to ground) to reject positive ions coming from the plasma. The bottom grid was swept from 0 to -1000 V with a step size of 10 V. A picoammeter biased at +30 V was used to collect the electron current. The positive bias on the collector was critical to suppress SEs emitted from the collector under bombardment by high-energy electrons. The resolution (full width at half maximum) of the electron energy analyzer was estimated to be $\sim 1.5\% - 2.0\%$ ($\Delta E/E$).¹⁰ The electron current density to the rf electrode was calculated from the measured collector current accounting for the mesh transparencies. The ion current to the dc electrode was recorded by the dc power supply.

Possible channels to produce BEs in the dc/rf hybrid are schematically shown in Fig. 2. For illustrative purposes, Fig. 2 shows a rf waveform on the substrate electrode having a peak-to-peak voltage ($V_{p,p}$) of 2100 V and a self-bias ($V_{\text{self-bias}}$) of -1000 V. The plasma potential (V_p) oscillates between just above the peak rf voltage and just above ground. These waveforms correspond to a 50 mTorr, 850 W rf, -800 V (V_{dc}) argon discharge (conditions used in Fig. 3). The secondary electron yield (SEY) of Al under 400–1000 eV Ar^+ ion bombardment is in the range of 0.08–0.12.¹¹ The SEY of Al under 50–2000 eV electron bombardment is in the range of $\sim 1 - 2$.¹² The SE emission characteristics are weakly dependent on the energy of the primary impinging particles but are strongly affected by the surface condition such as cleanliness and morphology.¹³ Due to the much higher SEY arising from electron bombardment, the contribution of sec-

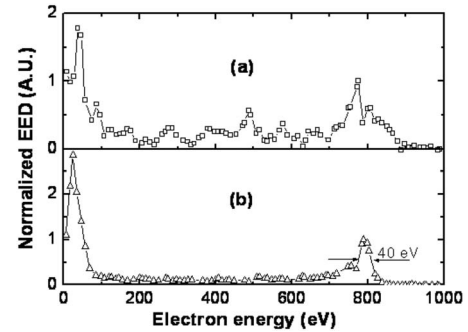


FIG. 3. EEDs with -800 V on the dc electrode: (a) electrons escaping (dumped) to the rf electrode (detected by analyzer A); (b) bulk plasma electrons (detected by analyzer B). The distribution functions are normalized using the corresponding peak at 800 eV. rf power was 850 W and discharge pressure was 50 mTorr.

ondaries due to electron bombardment should not be neglected in the dc/rf hybrid.

As illustrated in Fig. 2, when energetic Ar^+ ions impact the dc electrode, SEs are ejected and are accelerated across the dc sheath. At 50 mTorr, the mean free path for electron impact Ar atom ionization by 800 eV electrons is ~ 6 cm, which is comparable to the interelectrode gap (3 cm). Although a small portion of BEs loses energy to ionizing the gas (~ 20 eV for argon),¹⁴ these electrons remain highly energetic even after crossing the plasma bulk. BEs can overcome the sheath next to the rf electrode only when the instantaneous rf potential (V_{rf}) is more positive than -800 V (loosely termed as the “BE dumping” period in Fig. 2). BEs arriving at the rf electrode can knock out SEs, forming a lower-energy (< 800 V) BE beam that is unable to reach the -800 V dc electrode. During the rest of the rf cycle, when V_{rf} is higher than -800 V (termed as the “BE trapping” period in Fig. 2), BEs having energy below 800 eV are trapped in the plasma. Similarly, as energetic Ar^+ ions impinge the rf electrode, SEs could launch from that electrode. During the BE dumping period electrons emitted from the rf electrode cannot reach the dc electrode. However, during the BE trapping period, electrons emanating from the rf electrode ($\sim 800 - 2100$ eV) have enough energy to strike the dc electrode and produce further SE emanating from that electrode.

Analyzer A detects electrons during the BE dumping period and measures their energy with respect to ground potential. These should include SEs emitted from the dc electrode that strike the rf electrode. Analyzer B detects electrons from the plasma bulk. These should include SEs emanating from the dc electrode during the whole rf cycle. Figure 3 shows the electron energy distributions (EEDs) with -800 V applied to the dc electrode. Both analyzers clearly demonstrate the abundance of high-energy electrons (> 100 eV) in the dc/rf hybrid reactor. The energy spectra show a distinct peak at ~ 800 eV, indicating that a considerable fraction of secondaries was born on the dc electrode surface biased at -800 V. Electrons with energy from 100 to 700 eV could result from SE emission from the rf electrode under energetic electron or ion bombardment during the BE dumping period. This group of electrons could also be populated by 800 eV beam electrons that have lost part of their energy through collisional (mainly during the BE trapping period) and non-collisional (e.g., plasma wave excitation) processes. The en-

ergy distribution of electrons striking the rf electrode has reproducible fine structure in the range of 100–700 eV (top curve in Fig. 3). In contrast, this fine structure is not pronounced for analyzer B. Unlike analyzer A, the 800 eV peak dominates over the population of electrons in the 100–700 eV region for analyzer B, since BEs are sampled by that analyzer during the entire rf cycle. The wider high energy (around 800 eV) peak of analyzer A may be due to the oscillation of the rf sheath potential and gas phase collisional energy loss. In the case of analyzer B, electrons do not see the oscillating sheath potential, and the high energy peak is not as wide. The width of the high energy (around 800 eV) peak of analyzer B is likely determined by ~ 40 V rf ripple (higher harmonics) on the dc electrode.

For both analyzers, a distinct energy peak is located at about 30 eV extending to ~ 100 eV. The highly enhanced electron population in this energy range is consistent with the electron energy distribution function (EEDF) predicted by particle-in-cell (PIC) simulations at the same plasma conditions.⁶ This high-energy tail of the EEDF should be responsible for enhanced ionization, resulting in higher plasma densities. Landau damping of plasma waves is thought to be the main channel of the population growth of this energy group.¹⁵ Since BEs are largely collisionless and the beam density (n_b) was estimated (from the electron current collected by the analyzers) to be of the order of 10^7 cm⁻³, direct ionization by BE alone cannot explain the approximately four times increase in plasma density when the -800 V dc bias is applied (see below). It is known that Langmuir waves can be excited by a collisionless electron beam.^{15–18} The excitation process can be described as inverse Landau damping.¹⁸ The Langmuir waves excited initially ($\omega \geq \omega_p$) have high phase velocity near that of the BE beam. Therefore, these waves cannot transfer energy directly to the tail of the EEDF via Landau damping. However, the primary waves can be converted to ion density waves and SE waves such that the phase velocity of the secondary waves is near the speed of the tail of the EEDF, thus enabling energy transfer to the tail via Landau damping.^{15,16,19,20}

The EEDs measured in this work have some similarities with those in low current dc discharges^{21,22} measured with a detector behind a pinhole on the anode. The low energy part of the EED in those measurements was attributed to electrons backscattered from the anode and SEs emitted from the anode. However, the anode sheath in those measurements was a low voltage stationary sheath. In contrast, in the present work, the sheath over the rf electrode is a high voltage oscillating sheath resulting in more complex dynamics.

Under the conditions of 700 W rf and 50 mTorr, the ion flux to the dc electrode increased from 0.4 to 1.6 mA/cm², while the BE (>100 eV) flux dumped to the rf electrode increased dramatically from very low values to ~ 1.4 mA/cm², as the dc voltage was raised from -50 to -800 V. The increase in ion current reflects an increase in plasma density (and possibly electron temperature) at a

higher BE beam energy. Interestingly, at -800 V, the BE current is comparable to the ion current on the dc electrode. Since the SEY of 800 eV argon ions is ~ 0.1 , the BE current should be roughly ten times smaller than the ion current. Thus, the notion that SE emission from the rf electrode and the production of further secondaries from electron bombardment described in Fig. 2 is reinforced.

In summary, BEs with maximum energy corresponding to the dc electrode voltage were experimentally confirmed in a dc/rf hybrid plasma reactor. The BE current density was much higher than that exclusively originating from ion bombardment of the dc electrode, implying that the combination of rf and dc opens new pathways to produce BEs. These highly directional electrons may alleviate charging of the bottom of high aspect ratio features etched in insulators.

The authors wish to thank Yohei Yamazawa, Kimihiro Higuchi, Masanobu Honda, and Kazuya Nagaseki for valuable discussions.

- ¹E. Kawamura, M. A. Lieberman, A. J. Lichtenburg, and E. A. Hudson, *J. Vac. Sci. Technol. A* **25**, 1456 (2007).
- ²E. Kawamura, A. J. Lichtenburg, and M. A. Lieberman, *Plasma Sources Sci. Technol.* **17**, 045002 (2008).
- ³W. T. Lai, C. J. Hwang, A. T. Wang, J. C. Yau, J. Liao, L. H. Chen, K. Adachi, and S. Okamoto, *Proceedings of the International Symposium on Dry Process* (Institute of Electrical Engineers, Japan, 2006).
- ⁴M. Honda, K. Yatsuda, and L. Chen, PS1-WeA9, American Vacuum Society International Symposium, Boston, MA, 2008.
- ⁵L. Chen, A. Koshiishi, and S. Okamoto, Northern California Chapter of American Vacuum Society Meeting of Plasma Etcher User Group, San Jose, CA, 2006.
- ⁶A. Ranjan, L. Chen, K. Denpoh, P. Venzek, V. M. Donnelly, and D. J. Economou, PS-ThP21, American Vacuum Society International Symposium, Seattle, WA, 2007.
- ⁷M. Watanabe, D. M. Shaw, and G. J. Collins, *Appl. Phys. Lett.* **79**, 2698 (2001).
- ⁸D. M. Shaw, M. Watanabe, H. Uchiyama, and G. J. Collins, *Appl. Phys. Lett.* **75**, 34 (1999).
- ⁹D. M. Shaw, M. Watanabe, H. Uchiyama, G. J. Collins, and H. Sugai, *Jpn. J. Appl. Phys., Part 1* **38**, 4590 (1999).
- ¹⁰Y. Sakai and I. Katsumata, *Jpn. J. Appl. Phys., Part 1* **24**, 337 (1985).
- ¹¹M. A. Lewis, D. A. Glocker, and J. Jorne, *J. Vac. Sci. Technol. A* **7**, 1019 (1989).
- ¹²F. Le Pimpec, R. E. Kirby, F. K. King, and M. Pivi, *J. Vac. Sci. Technol. A* **23**, 1610 (2005).
- ¹³A. V. Phelps and Z. Lj. Petrović, *Plasma Sources Sci. Technol.* **8**, R21 (1999).
- ¹⁴M. A. Lieberman and A. J. Lichtenburg, *Principles of Plasma Discharges and Materials Processing*, 2nd ed. (Wiley, New York, 2005).
- ¹⁵D. V. Rose, J. U. Guillory, and J. H. Beall, *Phys. Plasmas* **9**, 1000 (2002).
- ¹⁶F. F. Chen, *Introduction to Plasma Physics*, 1st ed. (Plenum, New York, 1974).
- ¹⁷S. Kainer, J. Dawson, and R. Shanny, *Phys. Fluids* **15**, 493 (1972).
- ¹⁸I. Siliin, R. Sydora, and K. Sauer, *Phys. Plasmas* **14**, 012106 (2007).
- ¹⁹P. Rolland, *Phys. Fluids* **8**, 2114 (1965).
- ²⁰P. Gopalraja and J. Forster, *Appl. Phys. Lett.* **77**, 3526 (2000).
- ²¹S. B. Vrhovac, S. B. Radovanov, Z. Lj. Petrović, and B. M. Jelenković, *J. Phys. D* **25**, 217 (1992).
- ²²S. B. Vrhovac, V. D. Stojanović, B. M. Jelenković, and Z. Lj. Petrović, *J. Appl. Phys.* **90**, 5871 (2001).